Journal of Physiology (1995), **485.3**, *pp.*739–752

Action of salicylate on membrane capacitance of outer hair cells from the guinea-pig cochlea

M. J. Tunstall, J. E. Gale and J. F. Ashmore*

Department of Physiology, School of Medical Sciences, University of Bristol, Bristol BS8 1TD, UK

1. The effect of salicylate on membrane capacitance and intracellular pH has been measured in isolated outer hair cells (OHCs) during whole cell recording. Cell membrane capacitance was measured using a lock-in amplifier technique.

2. Salicylate applied in the bath reduced the fast charge movement, equivalent to a voltage-dependent membrane capacitance, present in OHCs. Simultaneous measurement of membrane capacitance and voltage-driven cell length changes showed that salicylate reduced both together.

3. A small effect of salicylate on outward currents at 0 mV was observed. Sodium salicylate (5 mM) reduced the currents by 19% and another weak acid, sodium butyrate (10 mM), reduced outward currents in OHCs by 15%.

4. The ratiometric dye 2,7-bis(2-carboxymethyl)-5,6-carboxyfluorescein (BCECF) was used to measure pH_i changes in OHCs during weak acid exposure. Membrane capacitance and pH_i were measured simultaneously in OHCs exposed first to 10 mM sodium butyrate and then to 5 mM sodium salicylate. Although both compounds produced a similar reduction in pH_i, butyrate decreased the resting capacitance from a mean resting capacitance of 35 pF (at −30 mV) by 5·4 ± 2·1 pF, whereas salicylate decreased it by 15·7 ± 2·3 pF ($n = 4$).

5. Exposure of OHCs to 10 mM sodium benzoate, an amphiphilic anion, reduced resting membrane capacitance at −30 mV by 9·2 ± 3·2 pF ($n = 3$). Outward currents, measured at 0 mV, were reduced by 0·25 ± 0·05 nA during benzoate application, comparable with the effect of salicylate.

6. Capacitance was measured during slow bath application of salicylate. The resulting dose–capacitance curve had a Hill coefficient of 3·40 ± 0·85 ($n = 4$) and a half-maximal dose of 3·95 ± 0·34 mM. The dose–capacitance curve was not significantly voltage dependent.

7. Salicylate had no detectable effect on the resting capacitance of Deiters' cells, a non-sensory cell type of the organ of Corti.

8. It is concluded that many of the described effects of salicylate on hearing may arise from the partitioning of the salicylate molecule into the membrane of the OHC and consequent inhibition of OHC motility.

Acetylsalicylic acid (aspirin) has a number of reversible effects on the auditory system when administered at clinical doses. These effects include hearing loss and subjective tinnitus (Myers & Bernstein, 1965; Mongan, Kelly, Neiss, Porter & Paulus, 1973), the elimination of the tip region of single unit tuning curves from cochlear nerve fibre recordings (Evans & Borerwe, 1982), the reduction in the low-intensity evoked cochlear action potential (Puel, Bledsoe, Bobbin, Caesar & Fallon, 1989), a decrease in auditory filter selectivity (Carlyon & Butt, 1993) and the elimination of both spontaneous otoacoustic emissions (McFadden & Plattsmier, 1984) and evoked otoacoustic emissions (Long & Tubis, 1988). At the cellular level, aspirin also causes a swelling of the subsurface cisternae of the outer hair cells (Douek, Dodson & Bannister, 1983).

The precise site or sites where salicylate mediates its effects are unknown, but its role in reducing otoacoustic emissions strongly suggests an effect on the outer hair cells (OHCs). The OHCs are unique amongst cochlear cells in that they are motile and change length rapidly in response to changes

* To whom correspondence should be addressed.

in membrane potential (Ashmore, 1987). These fast voltage-dependent length changes allow OHCs to generate forces sufficient to distort the basilar membrane (Mammano & Ashmore, 1993) and so alter cochlear mechanics. A favoured hypothesis to account for the motility of OHCs is that there is a 'motor' protein present in the basolateral membrane (Holley & Ashmore, 1988; Kalinec, Holley, Iwasa, Lim & Kachar, 1992). With change in membrane potential the motor undergoes a conformational change, producing a change in the surface area of the cell and a change in cell length.

These length changes in OHCs are associated with a movement of charge in the membrane, which is evident as a voltage-dependent capacitance (Ashmore, 1989*a*; Santos-Sacchi, 1991). The most likely explanation is that the charge movement corresponds to the conformational changes of the OHC motor protein. Further evidence for a tight linkage between charge movement and cell force generation is derived from experiments in which OHCs are stretched and generate charge movements directly (Gale & Ashmore, 1994). Preliminary data show that salicylate at millimolar concentrations blocks the voltage-dependent charge movement in OHCs (Ashmore, 1989*b*) as well as cell motility (Shehata, Brownell & Dieler, 1991). These results suggest that salicylate could mediate some of its effects on hearing by a direct action on the OHC motor protein.

We investigate this proposal by measuring the changes in the electrical and mechanical properties of OHCs during exposure to salicylate *in vitro*. The action of salicylate on the voltage-dependent charge movement is measured from its action on the cell membrane capacitance, which is determined using a software lock-in amplifier. From such continuous measurements of membrane capacitance we show that salicylate and a related compound possessing a benzyl ring can reduce voltage-dependent capacitance and motility of OHCs independently of changes in cytosolic pH. From the Hill coefficient of the dose–response curve we suggest that the motor may be present as a unit with three or four effective binding sites.

METHODS

Preparation of outer hair cells

Methods of preparation followed procedures described previously (Housley & Ashmore, 1992). Briefly, adult albino guinea-pigs were killed by rapid cervical dislocation. The bullae were removed and the organ of Corti was dissected in standard saline (for composition, see below). The tissue was then bathed in 0·5 mg ml^{-1} trypsin (Sigma type IV) for 15 min before gentle mechanical dissociation. The cells were transferred to a 200 μl chamber, which was mounted on the stage of an inverted microscope (Nikon TMD). Cells were superfused by a gravity feed system using inlet switch valves (LFAA series, Lee Valve, Westbrook, CT, USA), solutions being admitted to the chamber via a single inlet at 10 $\mu l\ s^{-1}$ and removed by suction. Complete bath solution changes could be produced within 30 s. Except where stated, all experiments were performed at room temperature (20–24 °C).

Solutions

External and internal solutions were buffered with phosphate and had the following compositions (mM). External solution: NaCl, 142; KCl, 4; $CaCl_2$, 1·0; $MgCl_2$, 1·5; Na_2HPO_4, 8·0; and NaH_2PO_4, 2·0; internal solution: KCl, 144; $MgCl_2$, 2·0; Na_2HPO_4, 8·0; NaH_2PO_4, 2·0; and EGTA, 5·0. The osmolarity of the solutions was adjusted to 325 ± 3 mosmol l^{-1} with D-glucose, osmolarities being determined using a freezing point osmometer (Camlab, Cambridge, UK). The pH of external and internal solutions was adjusted to 7·3 using NaOH and KOH, respectively. In experiments using sodium butyrate, benzoate or salicylate, NaCl in the external solution was reduced to compensate for the additional Na^+.

Recording methods

Electrophysiological recordings were made with conventional patch clamp techniques using an Axopatch 1D amplifier (Axon Instruments, Foster City, CA, USA). Patch pipettes were pulled on a two-stage vertical puller (PP-83 Narashige, Tokyo, Japan) using 1·2 mm o.d. thin-walled borosilicate glass (GC 120TF, Clark Electromedical Instruments, Pangbourne, UK). Pipettes had internal tip diameters of 1·5–3 μm and resistances of 2–5 MΩ measured in the bath. Resistances increased to 5–8 MΩ under whole cell recording conditions. No active series resistance compensation was employed because the resulting distortion of the command signal would have increased complexity of the analysis. Pipette junction potential changes during drug application were less than 1 mV and were ignored. For capacitance measurements pipettes were coated with ski-wax (Toko, Switzerland) to minimize stray capacitance (Fuchs & Evans, 1990). Data were acquired with a CED 1401 laboratory interface (Cambridge Electronic Design, Cambridge, UK) and stored on hard disk for later analysis. Analysed data were exported to a spreadsheet (Fig.P, Biosoft, Cambridge, UK) to enable convenient graphical representation.

Capacitance measurements

Measurement of cell capacitance was done using a software implementation of a lock-in amplifier to measure phase and amplitude of the currents in response to a sinusoidal command (Neher & Marty, 1982). A 10 mV amplitude sinusoidal command was applied to the pipette at a fixed frequency. There was no significant difference in the measured voltage-dependent capacitance when frequencies between 600 Hz and 5·19 kHz were used. A 1·2 kHz sine wave was therefore adopted in all experiments described. The current signal was filtered at 2 kHz to reduce spurious noise and sampled at 19·2 kHz. The capacitance was determined from the phase and amplitude of the resultant current according to a published algorithm that makes allowance for the changing pipette series resistance (Fidler & Fernandez, 1989). This phase-tracking algorithm was implemented in software on a laboratory interface (CED 1401) (Ashmore, Gale & Tunstall, 1994). The algorithm is described below.

Capacitance measurement using 'phase tracking'

The change in membrane capacitance is based on a standard model circuit for cell recording, which is a simple *RC* membrane in series with a pipette of resistance R_s. Therefore, the impedance (Z) measured by the patch amplifier at a frequency $f = \omega/2\pi$ Hz is given by

$$Z(\omega) = R_s + R_m/(1 + j\omega R_m C_m), \quad (1)$$

where $j = \sqrt{-1}$, R_m is the membrane resistance and C_m the membrane capacitance. With a sinusoidal command, $V\exp(\omega t)$,

the current $i(\omega) = V/Z(\omega)$. Small changes in the values of the parameters R_s, R_m or C_m will change the (complex) current by

$$\delta i(\omega) = \frac{V}{-Z(\omega)^2}\{-j\omega(Z(\omega)-R_s)^2\delta C_m + (Z(\omega)-R_s)^2\delta R_m + \delta R_s\}. \quad (2)$$

Thus both phase and amplitude of the current will alter. As noted originally (Neher & Marty, 1982), changes in C_m alter the current, $i(\omega)$, 90 deg out of phase with changes in R_m. Further, since $(Z(\omega) - R_s)^2 = -1/(\omega R_m C_m)^2$ is purely real for sufficiently large values of ω, the phasors δR_s and δR_m are in parallel but point at 180 deg to each other. Once the direction of δR_s is known, the vector direction of δR_m and δC_m can be determined. The cell capacitance, C_m, was determined from

$$C_m = C_o + \delta C_m = C_o + A(\omega)\,\delta i(\omega)/V, \quad (3)$$

where $A(\omega)$ is the projection of $Z(\omega)^2/(j\omega(Z(\omega) - R_s)^2)$ into the direction perpendicular to the vector δR_s, $\delta i(\omega)$ is the increment in current in the same direction and C_o is the voltage-independent capacitance of the cell.

In the limit of large ω, $A(\omega) = (1 + R_s/R_m)^2/\omega$. $A(\omega) = A(\omega, V)$ is implicitly a function of membrane potential. Thus, measurement of the current vector yields the capacitance, once corrected by a factor of $(1 + R_s/R_m)^2$. A similar factor arises in measurements of gating charge movement in other tissues (cf. Huang & Santos-Sacchi, 1993). It can most easily be seen to arise because the full command potential is not applied to the cell capacitance as a result of the series resistance of the pipette, R_s. If R_m becomes smaller (e.g. at depolarized potentials), the current $\delta i(\omega)$ *overestimates* capacitance δC_m by a factor of $A(\omega, V)/A(\omega, -60$ mV). In practice, R_s/R_m was less than 0·1, and thus the correction could account for, at most, 20% of the capacitance reduction seen at depolarized potentials (see Results). The correction is less than 3% between −100 and −30 mV because of the near linear I–V relationship for cells there. Therefore, with the exception of Fig. 2, this correction was not applied, since in experiments on the effects of salicylate at constant holding potentials there was no significant alteration of R_m near the holding potential (see Results). In practice, the cell capacitance, $C_m(V)$, was obtained directly by computing the change of capacitance from eqn (3) relative to the capacitance at −60 mV.

The assumption that δC_m changes are orthogonal to δR_s changes is strictly true only at high frequencies ($\omega \gg 1/R_m C_m$). As evident from eqn (2), the departure from orthogonality is given by an error angle, $\phi_{error} = \pi - 2\arg(1 + j\omega R_m C_m)$. If ω is large, then $\phi_{error} = 0$. If the frequency is not sufficiently large, capacitance changes cannot be completely separated from conductance changes. However, taking as typical values for an OHC $R_m = 100$ MΩ, $C_m = 30$ pF (Housley & Ashmore, 1992), $\phi_{error} = 5{\cdot}9$ deg at 1 kHz and declines to less than 2 deg at a maximum measuring frequency of 5 kHz. This error was not detectable in these experiments.

Experimental procedure

The experimental protocol was as follows. Once stable whole cell recording conditions were established, the charging transient at −60 mV was cancelled. C_o was read from the slow capacitance compensation control of the patch amplifier. The δR_s vector direction was determined by switching a 500 kΩ resistor in series with the bath at the beginning of each set of sixty measurement periods. Each period used sixteen cycles of the current response to extract phase and amplitude, providing a temporal resolution, without software overhead, of one capacitance measurement per 15 ms.

The value of the projection constant $A(w)$ was determined by adjusting the capacitance control of the amplifier by 5 pF at the initial holding potential of −60 mV. The calibration was checked independently by using a defined model cell as well as by comparing the results with measurements made from the charging transient (see Results). The results agreed to within 5%. Voltage-dependent capacitance was measured by applying voltages summed with the sinusoidal command in 5 mV steps from −130 to +80 mV. After each step to a new potential, the whole cell current was allowed to settle to the new steady-state level for 40 ms before a capacitance measurement was made. Data were discarded if the baseline capacitance varied by more than 1 pF between the beginning and end of a run. Each run of forty-five capacitance measurements took between 1·6 and 4 s to complete, depending upon the host computer speed.

Measurement of fluorescence ratios

The details of the equipment used to measure fluorescence have been described briefly elsewhere (Kolston & Ashmore, 1992). OHCs were illuminated alternately by lights of wavelength 440 and 490 nm using narrow band interference filters (Ealing Electro-Optics, Watford, UK). The illumination was produced from a 75 W xenon arc lamp filtered to remove infrared. The light beam was directed onto a rotating disc, reflecting on half its area, which allowed the beam to pass alternately through 440 and 490 nm filters and thence through a light guide to the epifluorescence port of the microscope. Illumination levels were minimized to reduce dye photobleaching. A 510 nm long-pass dichroic mirror was used to reflect the incoming light up to a 40 × 1·3 NA oil-immersion objective (Nikon) which focussed the light onto the cells. The emitted light then passed through the same lens and dichroic mirror and was filtered by a narrow band 530 nm fluorescein filter.

The cell images were captured by a two-stage intensified CCD camera (Extended Isis-M, Photonic Science, Robertsbridge, UK) connected to a PC, which acted as a host for a network of seven T800 transputers on three plug-in boards (Quintek, Bristol, UK). The image processing software allowed up to eight areas of 10 000 pixels to be centred around the image and the average fluorescence to be calculated over the area every 40 ms for subsequent ratio calculation. In practice, the data described below required two windows, one centred on the cell and a second on the background within 20 μm of the cell membrane. Four of the transputers were configured to allow signal-processing and hard disk storage of data at frame-rate speeds thereby removing the need for a video-recorder. No further averaging of frames was performed at this stage. Fields were acquired at 50 Hz and each field corresponded to excitation at either 440 or 490 nm wavelengths; a maximum temporal resolution of 40 ms could be achieved. However, because of the lag in the camera phosphor, slower rates were usually necessary (typically one ratio every 80 ms). Background subtraction was performed on the ratio data. The minimum and maximum ratios of the fluorescence were 0·43 and 1·7, respectively, for this apparatus. When measuring capacitance and BCECF ratio changes together, timing markers were applied to both traces to allow the data to be synchronized during subsequent analysis.

In experiments where BCECF measurements were performed simultaneously with whole cell tight-seal recording, 2·5 μM BCECF-dextran (MW 10 000, Molecular Probes) was included in the intracellular solution. A stable fluorescence signal for pH_i was measured within 2–3 min after whole cell break-in.

The basis of ratiometric BCECF measurements has been described extensively elsewhere (Grynkiewicz, Peonie & Tsien, 1985). The ratio of the intensity of the emitted fluorescence at 490 nm to that at 440 nm provides a signal related to pH_i over the window. The imaging of the fluorescence of the cell provided no evidence for local pH_i 'hot spots' in these experiments. Outer hair cells do regulate pH_i (Ikeda, Saito, Nishiyama & Takasaka, 1992) and the difficulties in the calibration of pH_i are well known for cells where there is regulation of an acid load (e.g. Vaughan-Jones & Wu, 1990). For this reason only the ratio of fluorescence at 490 nm to that at 440 nm (f_{490}/f_{440}) is given. Nevertheless, calibration of pH_i using a variant of a method where a weak base (trimethylamine, TMA) and a weak acid (butyrate) was applied to the cell (Szatkowski & Thomas, 1986) indicated that the resting pH_i values in OHCs were close to 7·3.

Each reagent was applied in the bath until the fluorescence had reached a steady-state value. Complete recovery was allowed to occur between the application of reagents.

All values are given as means ± S.D. Curves generated by text equations were fitted to data by a Levenberg–Marquardt algorithm (Fig.P, BioSoft).

RESULTS

Effect of salicylate on whole cell currents

Whole cell currents were recorded from OHCs held at −50 mV. The most prominent effect of salicylate was a reversible reduction in the transient current observed at command onset and offset. Figure 1 shows a typical experiment. This transient current, which lasted for less than 2 ms, has been attributed to the gating charge movement associated with a conformational change of a motor in the outer hair cell basolateral membrane (Ashmore, 1989*a*, 1992; Santos-Sacchi, 1991). Subtraction of corresponding sets of whole cell current traces (Fig. 1*A*) showed that the main effect of salicylate was suppression of a fraction of the transient current (Fig. 1*B*). In the presence of salicylate, the current kinetics accelerated slightly over the initial 15 ms, so that a small (< 200 pA) inward current resulted in the difference trace. Thereafter, salicylate reduced outward current (see below).

The time integral of the transient current can be described as a charge transfer, $Q_T(V)$, across the membrane. The simplest description is one where the charge can be distributed between either side of the OHC membrane (Ashmore, 1989*a*; Santos-Sacchi, 1991; Iwasa, 1993). Thus the equilibrium charge distribution on the outer membrane surface can be described by a Boltzmann function:

$$Q_T(V) = Q_{max}/(1 + \exp(-b(V - V_0)). \quad (4)$$

Here Q_{max} represents the maximum charge transferred, V_0, the potential at which the charge is equidistributed and b is a constant which is a measure of the potential sensitivity of charge displacement. $b = ze\xi/k_BT$ is given in terms of the number, z, of elementary charges, e, displaced across a fraction, ξ, of the membrane, k_B is Boltzmann's constant and T absolute temperature.

Figure 1*C* shows that the maximum charge transfer, $Q_{max} = 2{\cdot}33$ pC in control solution. The charge transfers at 'on' and 'off' were approximately equal. The voltage dependence of the charge was given by $V_0 = +21{\cdot}7$ mV (eqn (4)) and the slope of the curve corresponded to 0·93 elementary charges transferred across the membrane. For comparison, a sample of cells analysed in the same manner yielded $V_0 = -0{\cdot}52 \pm 21{\cdot}5$ mV ($n = 8$) at command onset and $V_0 = 2{\cdot}0 \pm 10{\cdot}1$ ($n = 11$) at offset.

In the presence of 5 mM salicylate, Q_{max} was reduced to 0·43 pC, that is, to 18·5% of its control value. There was no measurable shift in the gating charge distribution and this will be addressed further below. Similar results were obtained in three other cells analysed in this way but, for reasons given below, the phenomenon was analysed by a different technique.

Cell capacitance changes in OHCs

Although the rapid transients are apparent in whole cell records (e.g. Housley & Ashmore, 1992), the analysis is computationally intensive. To investigate the action of salicylate on motile mechanisms in hair cells, the membrane capacitance was measured instead. Once the cell capacitance at different potentials is known, it can either be integrated with respect to membrane potential to give charge transfer or it can be used directly as an indicator of targeted drug action. Cell capacitance measurement provides the basis for all subsequent experiments described here. It has the advantage of allowing rapid changes of the OHC gating charge process to be followed. It also offers a good signal-to-noise ratio, since the capacitance is determined from a longer (15 ms) segment of data.

The apparent cell membrane capacitance, C_m, in a cell with a gating charge movement $Q_T(V)$ will therefore be given by:

$$C_m(V) = C_{mo} + \frac{dQ_T(V)}{dV}$$

$$= C_{mo} + \frac{bQ_{max}\exp(-b(V - V_0))}{(1 + \exp(-b(V - V_0)))^2}, \quad (5)$$

where C_{mo} is the voltage-independent membrane capacitance. Typical values are $V_0 = 0$ mV, $Q_{max} = 2$ pC, and $b = 0{\cdot}04$ mV^{-1} for a cell 60 μm long (Ashmore, 1990; Santos-Sacchi, 1991; Gale & Ashmore, 1994). These values in general depend on the site of origin of the cell in the cochlea. From eqn (5), the maximum value of the cell capacitance, C_m, is $C_{mo} + bQ_{max}/4$. For the values given, $bQ_{max}/4 = 20$ pF. Equation (5) shows that capacitance provides data about Q_{max}, V_0 and b, parameters which enter into the description of transient current. Equation (5) also predicts that the capacitance–voltage (C–V) curve for OHCs should be bell shaped.

Figure 2 compares the capacitance derived from the charging transient and the capacitance measurement using sinusoidal commands. Capacitance measurements from

sinusoidal and charging transient methods agree closely. The results using sinusoidal commands tended to exhibit broader $C-V$ curves. The half-width of the $C-V$ curve was generally greater when measured with sinusoidal currents (typically, $b = 0{\cdot}015$–$0{\cdot}035$ mV^{-1} using eqn (5)) than when measured from charging transients ($b = 0{\cdot}0328 \pm 0{\cdot}0045$ mV^{-1}; $n = 11$; range, $0{\cdot}027$–$0{\cdot}042$ mV^{-1}) derived from fits using eqn (4)).

Both methods showed a maximal capacitance that declined to an asymptotic value negative to −100 mV. The position of the peak was quite variable, however. The peak capacitance occurred at a potential of $-27{\cdot}8 \pm 21{\cdot}0$ mV ($n = 40$; range −55 to −3 mV). The peak was shifted significantly to more negative values compared with those obtained from transient charge movements. For the cell illustrated in Fig. 2, the peak capacitance occurred at −16·5 mV using sinusoidal commands, whereas that derived from the 'on' and 'off' gating charge movements occurred at −6·7 and −17·5 mV, respectively.

Effect of salicylate on OHC length changes and membrane capacitance

As well as reducing the transient current, salicylate blocked potential-driven OHC length changes (Ashmore, 1989*b*; Shehata, Brownell & Dieler, 1991). The effect was reversible. Figure 3 shows this effect when membrane capacitance and cell length were monitored simultaneously. Length changes were measured using a differential photosensor to detect cuticular plate motion relative to a pipette at the cell base (Ashmore, 1987). Figure 3*A* shows that the length changes were maximally sensitive to membrane potential at V_0 (i.e. where C_m was maximal), and a fit to the voltage-dependent length change could be

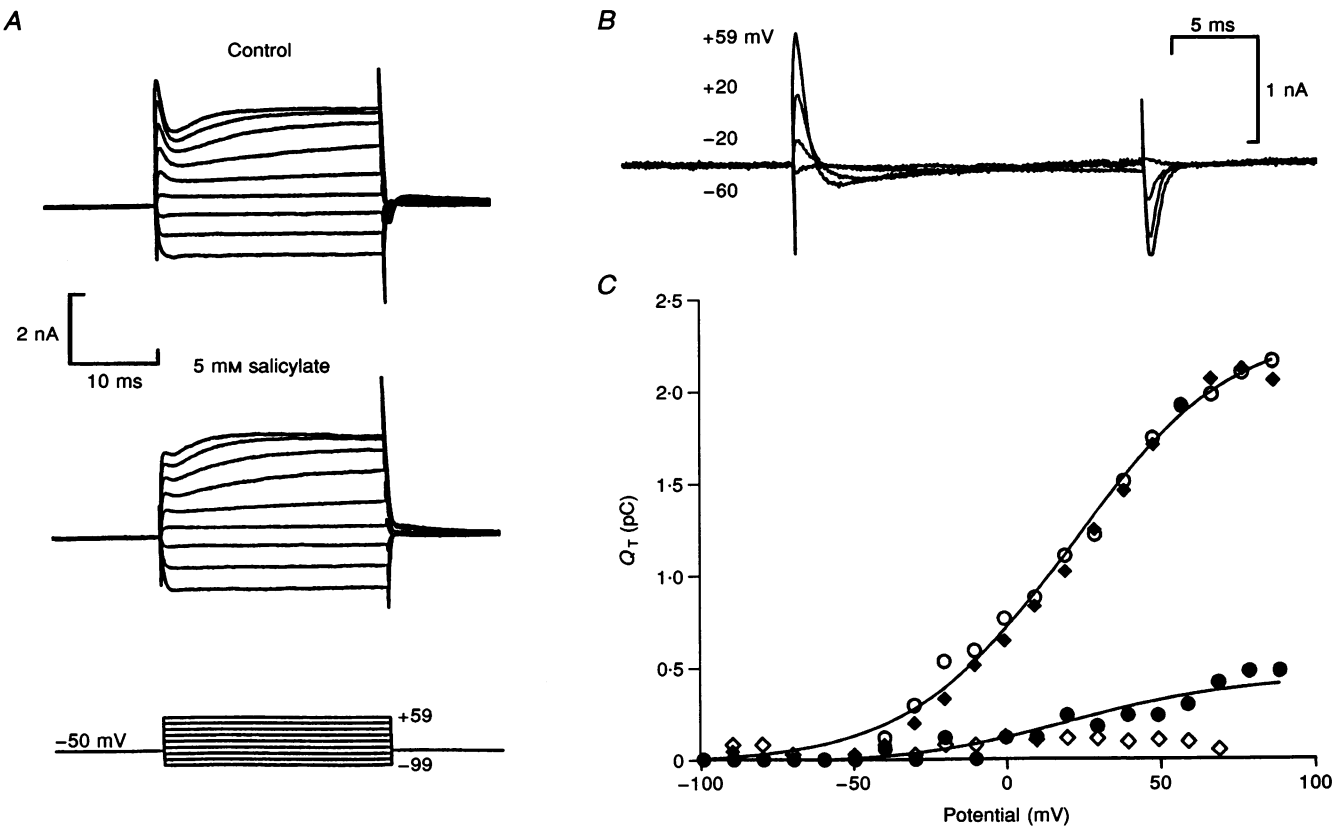

Figure 1. The action of salicylate on OHC currents

A, whole cell currents recorded from an OHC when stepped between −99 and +59 mV from a holding potential of −50 mV. Salicylate (5 mM) was bath applied. The transient currents at command onset and offset were reduced. Voltage stimulus is shown below. *B*, difference between currents (Control − salicylate) at potentials shown to left of traces. Because salicylate decreased the outward current at −50 mV, the baseline for these traces was 120 pA positive to 0. *C*, charge transfer in control conditions (○, ◆) and in the presence of 5 mM salicylate (●, ◇). The charge transfer, $Q_T(V)$, was determined by fitting an exponential to the transient current and integrating the area between it and the ionic currents. Diamonds, $Q_{T,\text{'off'}}$; circles, $Q_{T,\text{'on'}}$. Continuous curves, Boltzmann function (eqn (4)) fitted to data with parameters in control conditions: $V_0 = 21{\cdot}7$ mV, $b = 0{\cdot}037$ mV^{-1}, $Q_{max} = 2{\cdot}33$ pC; and in salicylate: $V_0 = 21{\cdot}7$ mV, $b = 0{\cdot}037$ mV^{-1}, $Q_{max} = 0{\cdot}43$ pC. A correction of 1·2 has been applied to Q_T at 'on' to provide the same normalization. Cell length, 65 μm.

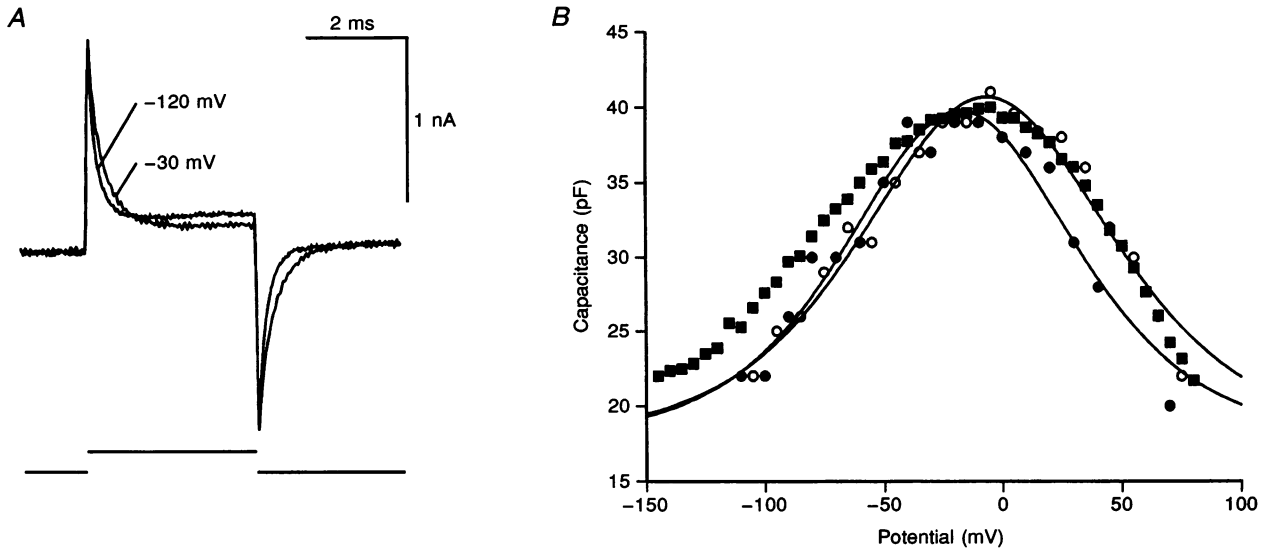

Figure 2. Comparison of cell capacitance using charging transient and lock-in amplifier methods

A, charging transients in response to 10 mV command step at −120 and −30 mV. The charging time constant at onset increased from 352 μs at −120 mV and to 820 μs at −30 mV. Holding current of cell subtracted. Pipette series resistance, 8·4 MΩ. *B*, capacitance derived from 'on' (○) and 'off' (●) of charging transients. The cell was held at −50 mV and stepped to potentials between −120 and +90 mV; after 6 ms, a 10 mV step was applied for 4 ms. Continuous lines, fit to off (on) data using eqn (5): $b = 0{\cdot}031$ $(0{\cdot}029)$ mV^{-1}, $V_0 = -17{\cdot}5$ $(-6{\cdot}7)$ mV, $C_{mo} = 18{\cdot}0$ $(18{\cdot}0)$ pF and $Q_{max} = 2{\cdot}76$ $(3{\cdot}04)$ pC. Capacitance measured using phase tracking method (■). The cell was stepped from −130 to +50 mV in 5 mV increments, each held for 200 ms. The fit using eqn (5) for these data was (curve not shown): $b = 0{\cdot}026$ mV^{-1}, $C_{mo} = 18{\cdot}9$ pF, $V_0 = -16{\cdot}4$ mV, $Q_{max} = 2{\cdot}58$ pC. Holding potential, −50 mV. Capacitance data corrected for R_m (see text). Cell length, 60 μm.

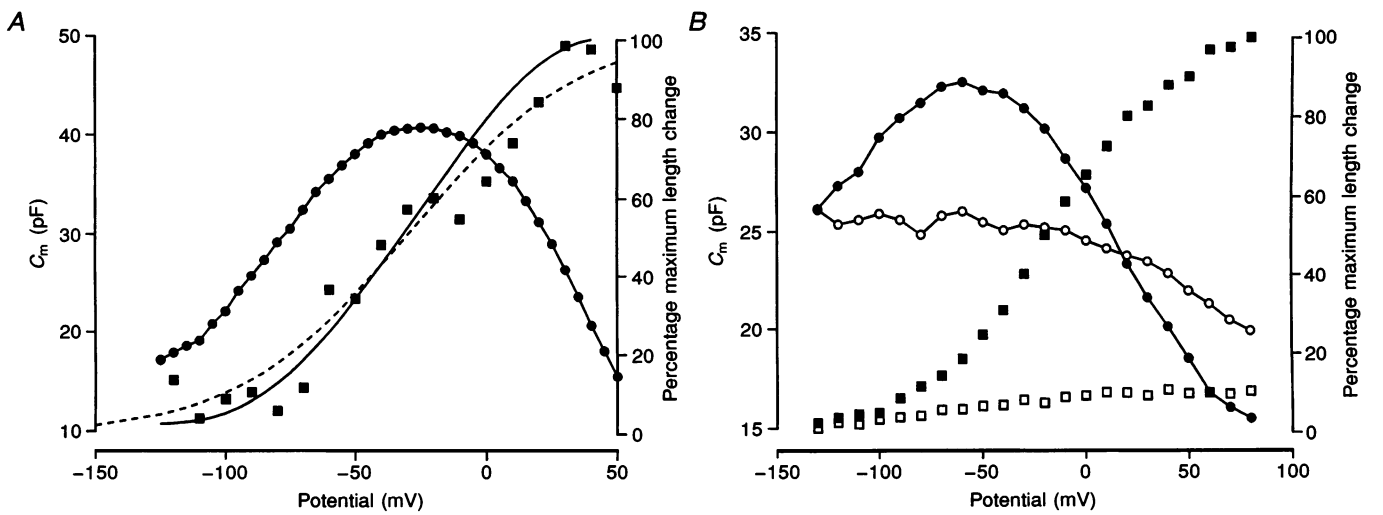

Figure 3. Salicylate reduces voltage-dependent cell capacitance and motility

A, cell capacitance (●) measured at same time as length change (■). Dashed line, Boltzmann curve fitted to length change, using $V_0 = -29{\cdot}3$ mV and $b = 0{\cdot}030$ mV^{-1}. Continuous curve, integral of capacitance relative to asymptote $C_{mo} = 16$ pF and normalized to maximum length change. Potential at half-maximum, −32 mV. *B*, effect of salicylate. Control cell capacitance (●) and length record (■) measured by a photosensor placed to measure axial length changes. Salicylate (5 mM) reduced the voltage-dependent capacitance (○) and length change (□). The length change was reduced to 10% of its control value. Maximal length change (Control), 2·5 μm. The additional decline in capacitance at potentials above 0 mV is discussed in the text. Cell length, 70 μm. The cell was held at −50 mV between test ramps.

obtained by integrating $C_m(V)$. Thus the change in cell length was, to a first approximation, proportional to the charge movement, $Q_T(V)$.

Figure 3*B* shows that bath application of 5 mM salicylate reduced the voltage-dependent OHC capacitance at potentials more negative than 0 mV. The measurements were made when the response to salicylate had reached a steady-state value. To a first approximation, the resulting curve was a simple rescaling of $(C_m - C_{mo})$. The residual capacitance in the presence of salicylate was 25 pF, which corresponded to 30% of the maximum voltage-dependent capacitance of a cell 60 μm long. In a sample of seven cells, 5 mM salicylate reduced the voltage-dependent capacitance to $28 \pm 14\%$ of its value at −50 mV (range, 0–44%). Above +20 mV there was a further reduction of membrane capacitance. The most probable explanation for this latter effect was distortion of the capacitance curves by activation of cell conductance (see Methods).

The reduction of voltage-dependent capacitance was matched by a reduction of length changes of the cell. Figure 3 shows that 5 mM salicylate also reduced the voltage-dependent length change in OHCs to 10% of its control value. Simultaneous measurements of capacitance and length in four other cells also produced comparable results. It can be concluded, therefore, that salicylate reduced the voltage-dependent capacitance and cell length changes between −100 and +50 mV. There was no evidence that salicylate acted by altering the voltage dependence of the charge movement as suggested previously (Ashmore, 1989*b*).

Effect of salicylate and butyrate on whole cell currents

Salicylic acid is a weak acid ($pK_a = 2{\cdot}9$) and permeates cell membranes. Given the strong pH dependence of many membrane proteins, it seemed possible that salicylate could exert its action through an interaction of H^+ ions with the motor proteins in the OHC plasmalemma. It might therefore be suggested that most of the effects on cell motility, the charging transient and whole cell currents were due to cytoplasmic acidification.

Salicylate (5 mM) produced a small alteration in the kinetics of outward currents (Fig. 1). It also caused a reduction of $0{\cdot}23 \pm 0{\cdot}02$ nA ($n = 4$; equivalent to a 19% reduction) in the steady outward currents measured at 0 mV when cells were matched for length (60–70 μm long). Although some recovery always occurred following salicylate removal, the extent varied between cells. In the cell illustrated in Fig. 4*A*, recovery was still incomplete when measured 30 min after removal of salicylate.

To act as a control for the action of salicylate on pH_i, the effects of another weak acid, butyrate ($pK_a = 4{\cdot}81$), were studied. The effect of 10 mM butyrate on steady currents was almost identical to that of 5 mM salicylate (Fig. 4*B*). Butyrate decreased currents (at 0 mV) by $0{\cdot}21 \pm 0{\cdot}03$ nA ($n = 4$). This was equivalent to a reduction of 15% of the outward current at 0 mV. This suggests that the effect on currents may be related primarily to the decrease in pH_i. In contrast to salicylate, recovery from butyrate exposure occurred far more readily. Recovery occurred 3–6 min after return to control conditions.

Effect of weak acids on pH_i and $C_m(V)$ measured simultaneously

To investigate whether the inhibition of OHC motility occurred through a change in pH, pH_i and $C_m(V)$ were

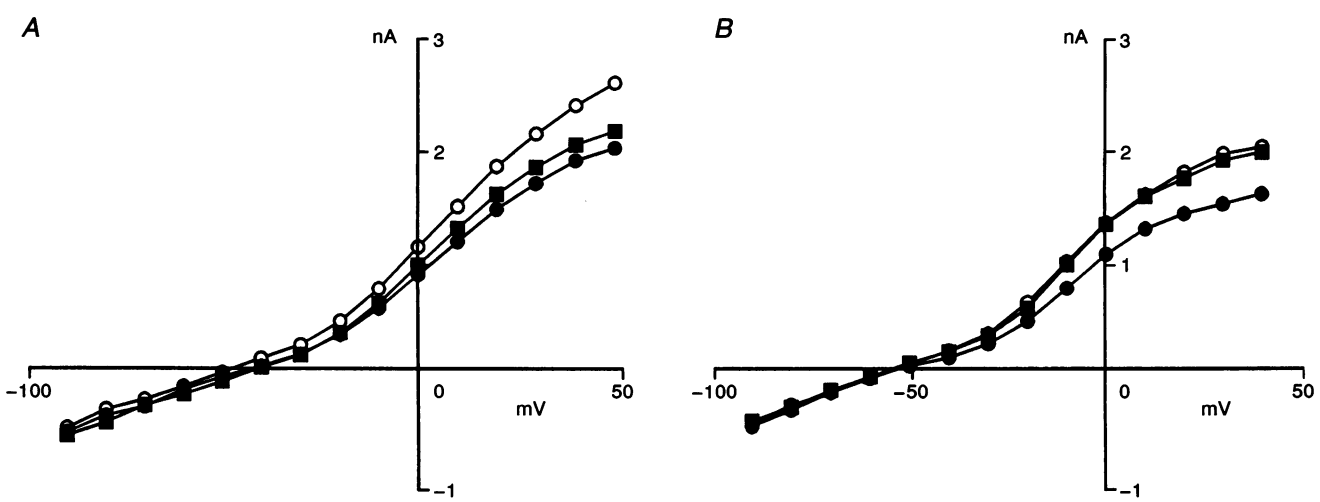

Figure 4. Effects of salicylate and butyrate on OHC steady-state current–voltage curves

○, control; ■, recovery. *A*, 5 mM sodium salicylate (●); *B*, 10 mM sodium butyrate (●). Reduction in currents at 0 mV: 0·242 nA (*A*); 0·18 nA (*B*). Current–voltage curves were obtained by stepping the cell for 100 ms to potentials from holding potential, −50 mV. Both salicylate and butyrate were bath applied. Measurements were made in steady-state conditions 50 ms after command onset. Cell length: 55 μm (*A*); 66 μm (*B*).

measured at the same time. The ratiometric fluorescent dye BCECF was used to estimate any cytoplasmic pH_i changes, a reduction in pH being signalled by an increase in the f_{490}/f_{440} ratio. Whole cell records were obtained with patch pipettes containing 10 μM BCECF-dextran added to the normal intracellular solution. The bath was perfused with 10 mM butyrate and then, following recovery of pH_i and capacitance, with 5 mM salicylate (Fig. 5*A*). Application of 10 mM butyrate and 5 mM salicylate caused an equivalent change in the BCECF ratio, indicating that the solution decreased pH_i by the same amount. In the four cells where simultaneous measurements were completed, the resting capacitance of the cells at −50 mV decreased by 13·6 ± 4·5 pF (5 mM salicylate) and by 4·3 ± 1·8 pF (10 mM butyrate). In one cell butyrate caused no capacitance change even though salicylate and butyrate

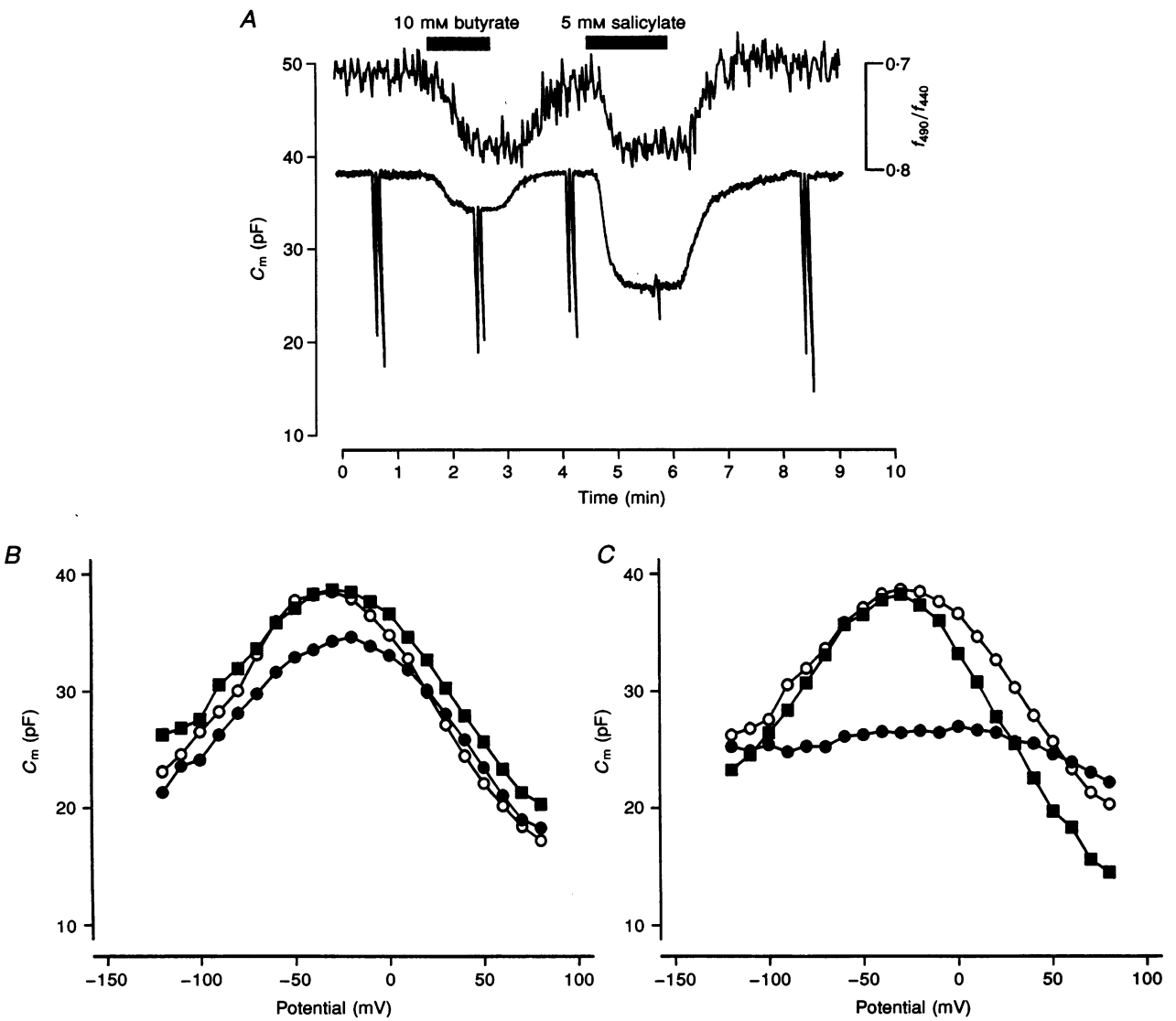

Figure 5. Salicylate inhibits voltage-dependent capacitance independently of changes in pH_i

A, similar changes in BCECF ratio induced by 10 mM butyrate and 5 mM salicylate (upper trace). Salicylate caused an approximately 3-fold larger decrease in the resting capacitance measured simultaneously, which fell from approximately 38 to 26 pF (lower trace). The large transient excursions in the capacitance trace here and in Figs 6 and 9 are capacitance changes produced by series of potential increments from −130 to +80 mV. The BCECF ratio is plotted as for conventional pH, i.e. acidification is downwards. Calibration of the ratio indicated that pH_i at rest was approximately 7·3 and fell to 6·9 on application of 5 mM salicylate. Capacitance–voltage curves for 10 mM butyrate (●, *B*) and 5 mM salicylate (●, *C*) taken from voltage ramps applied during the trace in *A*. ○, control; ■, recovery (*B* and *C*). The voltage-dependent capacitance was reversibly blocked by salicylate and there was a shift of the capacitance curve during butyrate application in this experiment. Cell length, 65 μm; holding potential, −50 mV.

produced identical increments of the BCECF ratio. Recovery of membrane capacitance to control values occurred between 2 and 6 min after return to control solution.

Comparison of salicylate and benzoate on OHC capacitance

To investigate whether the structure of salicylate might contribute to the reduction of cell capacitance, sodium benzoate was applied to the cell. Benzoate is an aromatic carboxylic acid with a chemical structure which differs from salicylate only in that it lacks a hydroxyl group attached to the benzyl ring.

Figure 6*A* shows that capacitance changes in response to 10 mM benzoate result in the resting capacitance being decreased by 9·2 ± 3·2 pF ($n = 3$) at −50 mV. Although benzoate also produced a reduction in pH (data not shown), the reduction in the voltage-dependent capacitance (Fig. 6*B*) was significantly larger than that produced by butyrate (Students's t test, $P < 0{\cdot}05$).

Figure 6*C* shows that exposure to 10 mM benzoate decreased whole cell currents by 0·25 nA at 0 mV (a 15% reduction, $n = 2$). Partial recovery occurred in 2–3 min following wash-out, but no further change occurred after a further 6 min.

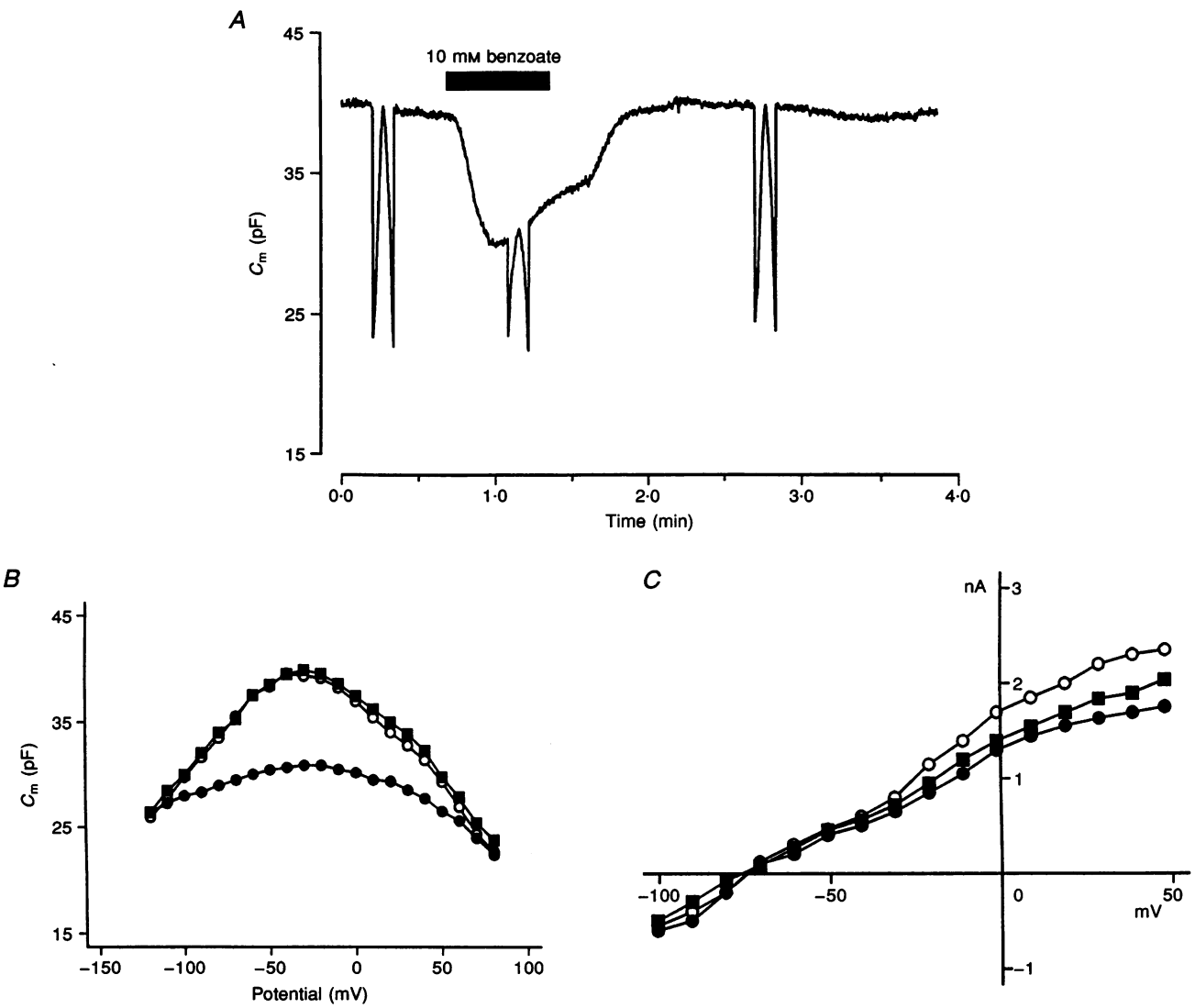

Figure 6. Effect of sodium benzoate on whole-cell currents and capacitance

A, 10 mM sodium benzoate caused a reversible decrease in the resting capacitance of 10·6 pF at −30 mV. *B*, reversible reduction of the voltage-dependent capacitance. *C*, decrease of whole-cell currents from 1·8 to 1·3 nA measured in steady-state conditions at 0 mV. Only a partial recovery occurred after 10 min on return to control conditions in this experiment. ○, control; ■, recovery; ●, 10 mM benzoate (*B* and *C*). Cell length, 55 μm; holding potential, −50 mV.

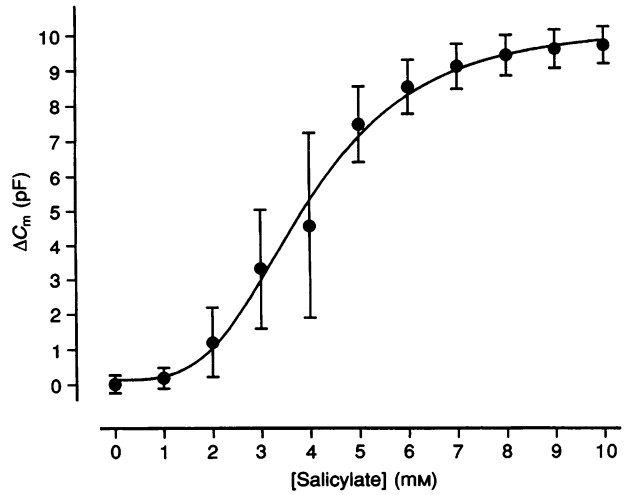

Figure 7. Dose–response curve for the effect of salicylate on capacitance

Data were pooled from 4 cells whose lengths ranged from 50 to 70 μm; they were matched for capacitance at −50 mV. The ordinate is the reduction in resting capacitance occurring during exposure to 10 mM salicylate. Cell holding potential, −50 mV; S.D. shown by bars. The smooth curve, relating ΔC_m, the reduction in capacitance to extracellular salicylate concentration, is eqn (6) with the Hill coefficient, $n_H = 3{\cdot}40$, and half-saturation, $K_m = 3{\cdot}95$. Curve fitting was performed using the Levenberg–Marquardt algorithm.

Thus, sodium benzoate is also capable of reducing capacitance in OHCs, suggesting that a common feature of the salicylate and benzoate molecules, such as the benzyl ring, may be important for their activity.

Dose–response curve for salicylate

To measure the dose–response curve for the effect of salicylate on capacitance, the concentration of salicylate in the bath near the cell was monitored by adding 10 μg ml^{-1} fluorescein isothiocyanate (FITC)-dextran (MW 10 000) to the 10 mM salicylate solution. This concentration of the indicator had no effect by itself on the whole cell currents. The flow rate in the bath was reduced by 5 times so that salicylate was able to equilibrate at each bath concentration. The salicylate concentration in the bath was monitored by measuring the change in fluorescence when flourescein was excited at a single wavelength of 440 nm. Whole cell recordings were made and capacitance monitored during the application of salicylate. The dose–capacitance curve was sigmoidal.

The reduction, ΔC_m, in membrane capacitance, C_m, at −50 mV could be fitted by a co-operative binding model:

$$\Delta C_m = C_{max}/(1 + ([\text{salicylate}]/K_m)^{n_H}), \quad (6)$$

where C_{max} is the maximum reduction in capacitance at −50 mV, K_m is the half-saturating concentration of salicylate and n_H is the Hill coefficient. Good fits to the data were obtained with half-saturation at $K_m = 3{\cdot}95 \pm 0{\cdot}34$ and $n_H = 3{\cdot}40 \pm 0{\cdot}85$ ($n = 4$) (Fig. 7). The best fit value, $C_{max} = 10{\cdot}4$ pF, obtained for the data was typical of values for the non-linear component of the OHC capacitance at −50 mV (see Fig. 2).

To investigate whether the salicylate inhibition of the dose–capacitance curve was voltage dependent (i.e. whether K_m or n_H in eqn (6) depend on membrane

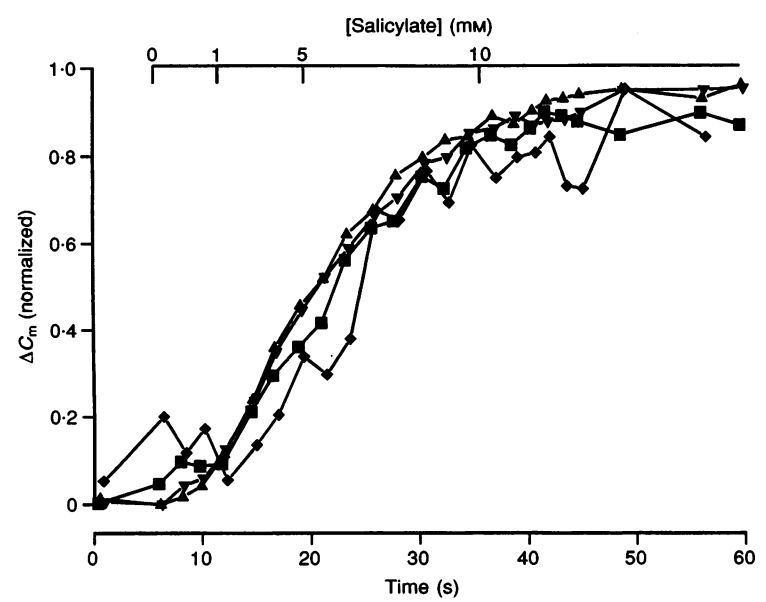

Figure 8. Salicylate inhibits capacitance independently of membrane potential

During slow superfusion of the bath with salicylate, the cell potential was stepped repetitively between −100, −50, 0 and +50 mV, repeating the cycle every 2 s. The separate capacitance curves, normalized, match. Holding potential, −50 mV. Initial capacitance: 21 pF at −100 mV; 39 pF at −50 mV; 38 pF at 0 mV; and 19 pF at + 50 mV. Capacitance change, C_{max}: 4 pF at −100 mV; 22 pF at −50 mV; 21 pF at 0 mV; and 2 pF at 50 mV. Minimum capacitance of cell, C_{mo}, 17 pF. Superfusion time was converted to salicylate concentrations, shown above, using fluorescence growth.

potential), a set of dose–capacitance curves was constructed at several membrane potentials. In the experiment, the cell was stepped rapidly through a sequence of different holding potentials during application of salicylate. Although the total capacitance changes were different at different holding potentials, Fig. 8 shows that, once normalized, the reduction of capacitance followed the same time course when measured at −100, −50, 0 or +50 mV. The data strongly suggest that salicylate acts in a voltage-independent manner, since both K_m and n_H were unaffected by holding potential. In particular, the data suggest that it is likely to be the uncharged form, salicylic acid, which acts on the hair cell motor.

Capacitance measurements in other cell types

Of all the cells in the mammalian cochlea, only OHCs possess voltage-dependent motility and there have been no reports of other cells also exhibiting a voltage-dependent capacitance. As a control for the outer hair cell data, salicylate was applied to Deiters' cells and inner hair cells (IHCs).

Figure 9 shows that salicylate reduced the outward current in Deiters' cells by 0·24 ± 0·04 nA ($n = 3$) at +10 mV, i.e. by approximately 15%. In all cases, recovery occurred 3–4 min after return to control solutions. The voltage-dependent capacitance was measured in three Deiters' cells (Fig. 9*A*). Salicylate had no effect on the resting capacitance in Deiters' cells, which was found to be 36·5 ± 7·3 pF ($n = 3$). Coincidently, these values are comparable with the capacitance in OHCs and correspond to a membrane area of 3650 μm^2 (assuming a specific membrane capacitance of 1 $\mu F\ cm^{-2}$). Likewise, no voltage-dependent capacitance nor an effect of salicylate was measured in two inner hair cells (data not shown).

DISCUSSION

Measurement of the OHC motor properties via cell capacitance

Capacitance measurements based on sinusoidal analysis, whether implemented in hardware or software, provide a rapid method for investigating critical properties of outer hair cells. The method is identical to that used to measure femtofarad capacitance changes in cells undergoing membrane fusion events.

Nevertheless, Fig. 2 shows that there are subtle differences between the *C–V* curves obtained by such techniques and those obtained by computing the charge transfer during small potential steps: the curves obtained by measuring the response to sinusoidal stimuli were wider, the peak tended to be shifted to more negative potentials when measured in the same cell (cf. Fig. 2) and the capacitance often continued to fall below the asymptote, C_{mo} (cf. eqn (5)) when measured at potentials more positive than +20 mV. The shift of the curve obtained using sinusoidal stimuli has also been noted in experiments where 2 mM $CoCl_2$ and ionic channel blockers were present (Santos-Sacchi, 1991). The present experiments show that with normal ionic solutions around the basolateral membrane surface, such differences cannot be the result of the screening effect of divalent ions.

There are several possible explanations for the differences between the voltage dependence of capacitance derived from the two methods. These include: (1) interaction between conductance and capacitance channels in phase-tracking methods because the associated current vectors are not completely orthogonal; (2) the effects of a 10 mV amplitude sinusoidal signal, which would broaden the peak of the curve by measuring an average capacitance over a region of membrane potentials where the capacitance varied rapidly with potential; (3) the kinetics of the cell

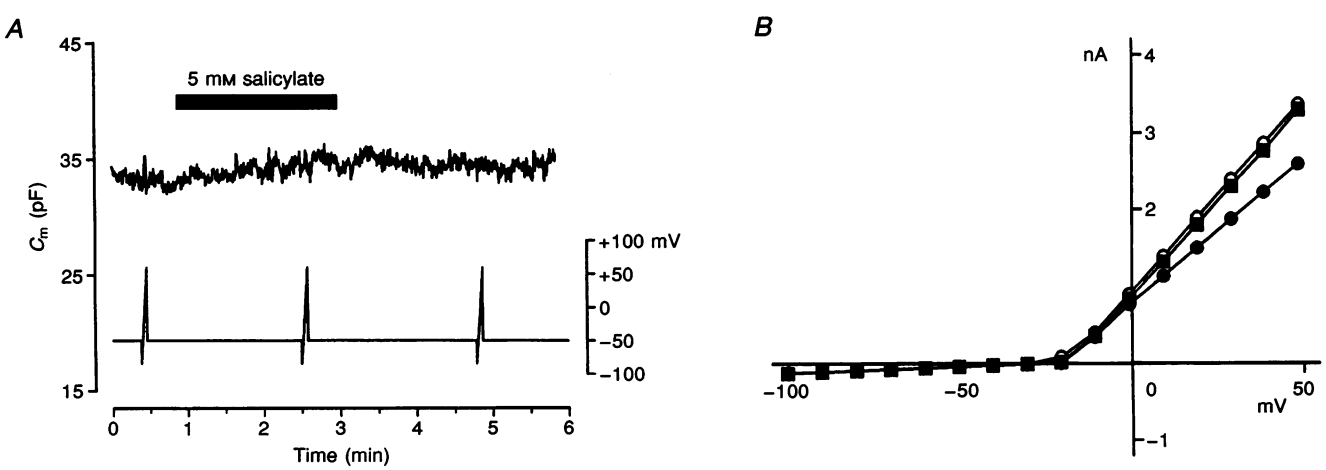

Figure 9. Effect of salicylate on Deiters' cells

A, when voltage was stepped from −130 to +80 mV there was no change in capacitance. Salicylate (5 mM) had no detectable effect on the resting capacitance. *B*, salicylate (5 mM; ●) reversibly reduced the outward currents at 0 mV by 0·13 nA. The outward current activated at −30 mV is a characteristic of Deiters' cells. ○, control; ■, recovery

conductance, which would tend to distort the C–V curve by adding a small reactive component to the capacitance channel; and (4) any change in cell input conductance, which will tend to decrease the estimated voltage-dependent capacitance (see Methods).

However, the most significant source of differences between the two methods is likely to arise from deactivation of the OHC charge movement. Immobilization of the gating charge has been been observed at negative potentials (Ashmore, 1989*a*; Santos-Sacchi, 1991) and there are differences in gating charge movement depending upon the experimental protocol. Capacitance has been measured here over a 15 ms interval, whereas step commands measure a single time constant in a 1 ms interval, usually after a negative prepulse. The effect of a negative prepulse appears to be to put the gating charge mechanism into an inactivated state and thus, during sinusoidal commands at a maintained potential around −50 mV, there will be a larger charge contributing to the apparent membrane capacitance. The effect would therefore be to broaden the C–V curve.

The mechanism of inhibition of OHC motility

The salicylate anion contains a benzyl ring and exhibits both hydrophilic and lipophilic properties. As salicylic acid, it permeates the cell membrane and dissociates to acidify the cell cytoplasm. This acidification is exhibited in experiments with BCECF-loaded cells, which show that $[H^+]$ rises throughout the cytoplasm. Unfortunately, imaging does not offer sufficient spatial resolution to identify changes near the motor site in the cell membrane. However, the reduction of outward current (Fig. 4) occurs over a potential range where calcium activated potassium ($K_{(Ca)}$) currents contribute to the OHC current–voltage curve (Housley & Ashmore, 1992). The current reduction is most readily explained by an interaction between protons and calcium at a regulatory site on the $K_{(Ca)}$ channel (Copello, Segal & Reuss, 1991). Thus, it appears that the cytoplasmic BCECF signal is also reporting elevation of $[H^+]$ near the cell membrane motor site. The independence of capacitance changes and BCECF ratio changes (Fig. 5) allows us to conclude that the intracellular $[H^+]$ elevation plays a minor role in the suppression of OHC motility.

The simplest explanation, therefore, for the effect on motility is that salicylate acts by partitioning into the cell membrane. In this manner salicylate could block the conformational changes in the proteins that appear to underlie motility (Kalinec *et al.* 1992; Ashmore, 1992). There are several arguments that support this conclusion.

The half-saturating salicylate concentration (3·95 mM) is a high value for binding of a ligand to an integral membrane protein where a K_m in the micromolar concentration range may be expected. For example, aspirin binds to cyclo-oxygenase 1 in bovine aortic endothelial cells with $IC_{50} = 2\ \mu M$ (Mitchell, Akarasereenont, Thiemermann, Flower & Vane, 1994). This case arises from a specific binding site in the cyclo-oxygenase molecule. The dose for the measurable action on OHCs is closer to that appropriate to red blood cells, where changes of morphology and a discocyte–echinocyte transformation are produced (Reinhart & Chien, 1986). The voltage independence of salicylate binding described above also suggests that the action of salicylate does not involve a voltage-dependent protein binding step, but is much more likely to act through an action on the lipid or at the lipid–protein interface.

An explanation for salicylate action in several tissues is that its amphiphilic nature produces charge screening effects (McLaughlin, 1973). This hypothesis suggests that salicylate partitions into the membrane and alters the membrane field experienced by membrane proteins. Salicylate levels in the low millimolar range can also, through this mechanism, distinguish between different modes of action of calcium channel antagonists (Spedding, 1984). Although the measurements of pH_i show that the OHC membrane is highly permeable to salicylate (presumably as the uncharged form, salicylic acid), there is little evidence in the present results for any surface charge effects. First, absorption of an anion onto the outer surface would be expected to shift the voltage dependence of the length change and the peak of the $C_m(V)$ curve to more hyperpolarized potentials. This was not observed. Second, there was no evidence for a voltage-dependent binding curve. Third, the motor protein is unlikely to be an ion channel (Ashmore, 1992) and the mode of action is unlikely to be the same as those described in reports on excitable tissues (McLaughlin, 1973).

The simplest explanation, therefore, is that salicylate and related compounds act on OHC motility when the molecule partitions into the membrane. The data cannot distinguish between salicylic acid acting as a uncharged molecule that interferes with the fluidity of the lipid environment of the motor protein, or the benzyl ring of salicylate entering the membrane and permitting the anionic side-group to combine with cationic binding sites on motor proteins. The voltage independence of binding indicates that, in the latter case, the interaction would have to be well screened from the electric field.

The dose–capacitance curve (Fig. 7) suggests that the co-operative action of three or four salicylate molecules is required to alter the OHC motor protein. To explain this observation, suppose that motor protein is packed sufficiently densely so that the molecule forms a close-packed array in which a basic repeat is a tetramer. It has been proposed that reorientation of such a tetrameric array occurs when the membrane potential changes (Kalinec *et al.*

1992). If the charge movement in the OHC basolateral membrane is indeed dependent upon a 'unit' that is a cluster of four molecular subunits, then the apparent stochiometry of the salicylate inhibition of capacitance (and therefore length change) suggests that each subunit must bind a salicylate molecule before inhibition occurs.

There has been another report of the effects of salicylate which show that at millimolar extracellular levels it can reduce isolated OHC motility (Shehata *et al.* 1991). This report also described considerable disruption of the lateral cisternae with the doses used. Since such changes were reported after incubation of OHCs at 37 °C for 15 min it seems possible that the effects described there were a result of the acidification of the cell rather than due to membrane effects. The reported irreversible increase of cell input conductance and reduction of the zero current potential must be seen as an extreme form of the reversible changes observed here.

Action of salicylates on hearing mechanisms

OHCs shorten in response to depolarization and lengthen in response to hyperpolarization. These changes are rapid, occurring within the first 100 μs of the imposed voltage step (Ashmore, 1987; Santos-Sacchi, 1991). The role proposed for OHCs in cochlear operation has been one where the cells provide local mechanical enhancement of the cochlear partition in response to a stimulus delivered to their stereocilia. In recent experiments where the whole cochlear partition was stimulated by transverse electric current and the OHC basolateral membrane polarized, it was shown that the OHCs produce sufficient forces to distort the basilar membrane (Mammano & Ashmore, 1993). These mechanical forces were reversibly reduced by superfusion with 10 mM sodium salicylate. The explanation offered for that result was that salicylate directly inhibited the OHC motor. The data here support this view.

There are further measurable actions of ingested aspirin on hearing which have been reinvestigated recently. These include broadening of psychoacoustic tuning curves (Carlyon & Butt, 1993) and reduction of the distortion products measured in the ear canal (Brown, Williams & Gaskill, 1993). Although there are no models of cochlear function which can quantitatively explain otoacoustic emissions and non-linear phenomena, it is possible to provide a qualitative explanation for most of these observations if the OHC motor alone is affected, even though there are indications that further ototoxic effects may arise indirectly through salicylate effects on cochlear blood flow (Didier, Miller & Nuttall, 1993). There is ample evidence to suggest that aspirin ingestion leads to elevated serum salicylate levels, in some cases in the millimolar range (Jastreboff, Hansen, Sasaki & Sasaki, 1986). These levels are not cleared rapidly and may distribute between serum, cerebrospinal fluid and perilymph. The effects of aspirin on hearing are observed only after steady aspirin absorption, typically over 24 h. It seems reasonable to assume, therefore, that the levels of salicylate in the inner ear may reach the low millimolar levels described here and that the effect is to remove the OHCs from their role as force feedback elements in cochlear mechanics.

Ashmore, J. F. (1987). A fast motile response in guinea-pig outer hair cells: the cellular basis of the cochlear amplifier. *Journal of Physiology* **388**, 323–347.

Ashmore, J. F. (1989*a*). Transducer motor coupling in cochlea outer hair cells. In *Cochlear Mechanisms: Structure, Function and Models*, ed. Wilson, J. P. & Kemp, D. T., pp. 107–114. Plenum Press, New York.

Ashmore, J. F. (1989*b*). Effect of salicylate on a rapid charge movement in outer hair cells isolated from the guinea-pig cochlea. *Journal of Physiology* **412**, 46*P*.

Ashmore, J. F. (1990). Forward and reverse transduction in the mammalian cochlea. *Neuroscience Research* suppl. 12, 539–550.

Ashmore, J. F. (1992). Mammalian hearing and the cellular mechanisms of the cochlear amplifier. In *Sensory Transduction*, ed. Roper, S. & Corey, D. P., pp. 395–412. Rockefeller University Press, New York.

Ashmore, J. F., Gale, J. E. & Tunstall, M. J. (1994). Measurement of cell capacitance using a CED1401 interface. *Journal of Physiology* **476.P**, 7*P*.

Brown, A. M., Williams, D. M. & Gaskill, S. A. (1993). The effect of aspirin on cochlear mechanical tuning. *Journal of the Acoustical Society of America* **93**, 3298–3307.

Carlyon, R. P. & Butt, M. (1993). Effects of aspirin on human auditory filters. *Hearing Research* **66**, 233–244.

Copello, J., Segal, Y. & Reuss, L. (1991). Cytosolic pH regulates maxi K^+ channels in *Necturus* gall-bladder epithelial cells. *Journal of Physiology* **434**, 577–590.

Didier, A., Miller, J. M. & Nuttall, A. L. (1993). The vascular component of sodium salicylate ototoxicity in the guinea pig. *Hearing Research* **69**, 199–206.

Douek, E. E., Dodson, H. C. & Bannister, L. H. (1983). The effects of salicylate on the cochlea of the guinea-pig. *Journal of Laryngology and Otology* **93**, 793–799.

Evans, E. F. & Borerwe, T. A. (1982). Ototoxic effects of salicylate on the responses of single cochlear nerve fibres and on cochlear potentials. *British Journal of Audiology* **16**, 101–108.

Fidler, N. & Fernandez, J. M. (1989). Phase-tracking: an improved detection technique for cell membrane capacitance measurements. *Biophysical Journal* **56**, 1153–1162.

Fuchs, P. & Evans, M. G. (1990). Potassium currents in hair cells isolated from the cochlea of the chick. *Journal of Physiology* **429**, 529–561.

Gale, J. E. & Ashmore, J. F. (1994). Charge displacement induced by rapid stretch in the basolateral membrane of the guinea pig outer hair cell. *Proceedings of the Royal Society* B **255**, 243–249.

Grynkiewicz, G. M., Poenie, M. & Tsien, R. Y. (1985). A new generation of Ca^{2+} indicators with greatly improved fluorescence properties. *Journal of Biological Chemistry* **260**, 3440–3450.

Holley, M. C. & Ashmore, J. F. (1988). On the mechanism of a high frequency force generator in outer hair cells isolated from the guinea pig cochlea. *Proceedings of the Royal Society* B **232**, 413–429.

Housley, G. D. & Ashmore, J. F. (1992). Ionic currents of outer hair cells isolated from the guinea-pig cochlea. *Journal of Physiology* **448**, 73–98.

Huang, G. & Santos-Sacchi, J. (1993). Mapping the distribution of the outer hair cell motility voltage sensor by electrical amputation. *Biophysical Journal* **65**, 2228–2236.

Ikeda, K., Saito, Y., Nishiyama, A. & Takasaka, T. (1992). Intracellular pH regulation in isolated cochlear outer hair cells of the guinea pig. *Journal of Physiology* **447**, 627–648.

Iwasa, K. H. (1993). Effect of stress on the membrane capacitance of the auditory outer hair cell. *Biophysical Journal* **65**, 492–498.

Jastreboff, P., Hansen, R., Sasaki, P. G. & Sasaki, C. T. (1986). Differential uptake of salicylate in serum, cerebro-spinal fluid and perilymph. *Archives of Otolaryngology* **112**, 1050–1053.

Kalinec, F., Holley, M. C., Iwasa, K. H., Lim, D. J. & Kachar, B. (1992). A membrane-based force generation mechanism in auditory sensory cells. *Proceedings of the National Academy of Sciences of the USA* **89**, 8671–8675.

Kolston, P. J. & Ashmore, J. F. (1992). Using computers to measure calcium changes in isolated cochlear cells. *Journal of Physiology* **452**, 170*P*.

Long, G. R. & Tubis, A. (1988). Modifications of spontaneous and evoked otoacoustic emissions and associated psychoacoustic microstructure by aspirin consumption. *Journal of the Acoustical Society of America* **84**, 1343–1345.

McFadden, D. & Plattsmier, H. S. (1984). Aspirin abolishes spontaneous otoacoustic emissions. *Journal of the Acoustical Society of America* **76**, 443–448.

McLaughlin, S. (1973). Salicylates and phospholipid bilayers. *Nature* **243**, 234–236.

Mammano, F. & Ashmore, J. F. (1993). Reverse transduction measured in the isolated cochlea by laser Michelson interferometry. *Nature* **365**, 838–841.

Mitchell, J. A., Akarasereenont, P., Thiemermann, C., Flower, R. J. & Vane, J. R. (1994). Selectivity of nonsteroidal anti-inflammatory drugs as inhibitors of constitutive and inducible cyclooxeganase. *Proceedings of the National Academy of Sciences of the USA* **90**, 11693–11697.

Mongan, E., Kelly, P., Neis, K., Porter, W. & Paulus, E. (1973). Tinnitus as an indicator of the therapeutic serum salicylate levels. *Journal of the American Medical Association* **226**, 142–145.

Myers, E. M. & Bernstein, J. M. (1965). Salicylate ototoxicity. A clinical and experimental study. *Archives of Otolaryngology* **82**, 483–493.

Neher, E. & Marty, A. (1982). Discrete changes of cell membrane capacitance observed under conditions of enhanced secretion in bovine adrenal chromaffin cells. *Proceedings of the National Academy of Sciences of the USA* **79**, 6712–6716.

Puel, J. L., Bledsoe, S. C., Bobbin, R. P., Caesar, G. & Fallon, M. (1989). Comparative actions of salicylate on amphibian lateral line and the guinea pig cochlea. *Comparative Biochemistry and Physiology* **93C**, 73–80.

Reinhart, W. H. & Chien, S. (1986). Red cell rheology in stomatocyte–echinocyte transformation: roles of cell geometry and cell shape. *Blood* **67**, 1110–1118.

Santos-Sachi, J. (1991). Reversible inhibition of voltage-dependent outer hair cell motility and capacitance. *Journal of Neuroscience* **11**, 3096–3110.

Shehata, W. E., Brownwell, W. E. & Dieler, R. (1991). Effects of salicylate on shape, electromotility and membrane characteristics of isolated outer hair cells from guinea-pig cochlea. *Acta Otolaryngolica* **111**, 707–718.

Spedding, M. (1984). Changing surface charge with salicylate differentiates between subgroups of calcium-antagonists. *British Journal of Pharmacology* **83**, 211–220.

Szatkowski, M. S. & Thomas, R. C. (1986). New method for calculating pHi from accurately measured changes in pHi induced by a weak acid and base. *Pflügers Archiv* **407**, 59–63.

Vaughan-Jones, R. D. & Wu, M.-L. (1990). pH dependence of H^+ intrinsic buffering power in the sheep cardiac Purkinje fibre. *Journal of Physiology* **425**, 429–448.

Acknowledgements

This work was supported by the Medical Research Council, the Hearing Research Trust and the European Community (ESPRIT SSS 6961). J.E.G. was a Hearing Research Trust/Colt Foundation student. We thank Dr P. J. Kolston for critical assistance with the development of the pH imaging system.

Author's present address

M. J. Tunstall: Department of Neurobiology and Anatomy, University of Texas Medical School, PO Box 20708, Houston, TX 77225, USA.

Received 15 March 1994; accepted 20 December 1994.